

Topographic Maps within Brodmann's Area 5 of Macaque Monkeys

Adele M. H. Seelke¹, Jeffrey J. Padberg², Elizabeth Disbrow^{1,3}, Shawn M. Purnell¹, Gregg Recanzone^{1,4} and Leah Krubitzer^{1,5}

¹Center for Neuroscience, University of California, Davis, Davis, CA 95616, USA, ²Department of Biology, University of Central Arkansas, Conway, AR 72035, USA and, ³Department of Neurology, ⁴Department of Neurobiology, Physiology and Behavior and ⁵Department of Psychology, University of California, Davis, Davis, CA 95616, USA

Address correspondence to Leah Krubitzer, University of California, Davis, Center for Neuroscience, 1544 Newton Court, Davis, CA 95616, USA.
Email: lakrubitzer@ucdavis.edu.

Brodmann's area 5 has traditionally included the rostral bank of the intraparietal sulcus (IPS) as well as posterior portions of the postcentral gyrus and medial wall. However, different portions of this large architectonic zone may serve different functions related to reaching and grasping behaviors. The current study used multiunit recording techniques in anesthetized macaque monkeys to survey a large extent of the rostral bank of the IPS so that hundreds of recording sites could be used to determine the functional subdivisions and topographic organization of cortical areas in this region. We identified a lateral area on the rostral IPS that we term area 5L. Area 5L contains neurons with receptive fields on mostly the shoulder, forelimb, and digits, with no apparent representation of other body parts. Thus, there is a large magnification of the forelimb. Receptive fields for neurons in this region often contain multiple joints of the forelimb or multiple digits, which results in imprecise topography or fractures in map organization. Our results provide the first overall topographic map of area 5L obtained in individual macaque monkeys and suggest that this region is distinct from more medial portions of the IPS.

Keywords: area 2, area 5, medial intraparietal cortex, posterior parietal cortex, primates

Introduction

Historically, there has been a great deal of contention over the status of Brodmann's area 5 (BA5) and how it should be subdivided. Initially, area 5 was described architectonically as a large wedge-shaped field caudal to area 2 in Old World monkeys (Brodmann 1909). This field encompasses the rostral or medial bank of the intraparietal sulcus (IPS) and extends onto much of the caudal portion of the postcentral gyrus, especially in the medial portion where area 5 is the widest. Medially, area 5 wraps onto the medial wall and borders the cingulate sulcus (Fig. 1A). In Brodmann's scheme, this large area 5 is bordered rostrally by somatosensory area 2 and posteriorly by area 7. Somewhat later architectonic schemes also defined this region in the location of BA5 but termed this region the parietal area, PE (e.g., von Economo 1929; von Bonin and Bailey 1947). Subsequently, there have been numerous architectonic studies utilizing both traditional and more modern histological techniques (e.g., Hof and Morrison 1995) to further define this large zone, and as a result both the extent and the boundaries of area 5/PE have been redefined and subdivided (e.g., PE, PEc, PEa, Seltzer and Pandya 1986 or areas 5d and 5v, Lewis and Van Essen 2000; Fig. 1B,D; for abbreviations, see Table 1).

Studies using single unit electrophysiological recording techniques to examine the functional properties of neurons in BA5 are highly variable in both the location in which the

recordings were made as well as the neuronal properties described. For example, in early single unit studies, most of the rostral bank of the IPS and the caudal portion of the postcentral gyrus was explored and considered to be area 5 (e.g., Sakata et al. 1973; Mountcastle et al. 1975), but the region explored did not include the lateral most portion of the IPS nor cortex on the medial wall (Fig. 2A,B). A number of subsequent electrophysiological studies reported recording from sites in area 5, but the location of the recording sites varied significantly across studies (e.g., Ferraina and Bianchi 1994; Iwamura et al. 1994; Kalaska 1996; Taoka et al. 1998, 2000; Gardner, Babu, Ghosh, et al. 2007; Gardner, Babu, Reitzen, et al. 2007; Chen et al. 2009; Fig. 2). Therefore, it is not surprising that the results and interpretations of the function of area 5 varied as well. Although, both architectonic and electrophysiological recording studies have divided this large traditional area 5 (Figs 1 and 2), the functional subdivisions do not appear to correspond well with architectonic subdivisions. Despite differences across studies, there is overwhelming evidence that areas in the IPS are involved in complex hand use, reaching, grasping, matching visual and body centered frames of references for reaching and grasping, and programming intentional hand movements.

Lesions of posterior parietal cortex in humans provide insight into the function of posterior parietal areas, and observations of deficits are consistent with results from studies in nonhuman primates. For example, lesions that incorporate cortex of the IPS and inferior and superior parietal lobule result in Balint's syndrome, which is characterized by severe optic ataxias or misreaching to visual targets as well as impaired spatial attention or hemi neglect (for review, see Caminiti et al. 2010). Lesions in humans that were limited to the medial bank of the IPS, which may include both area 5L and MIP/PRR, result in distinct manual deficits in visually guided goal-directed reaching (Trillenberget et al. 2007), while visually guided saccades were not effected. Interestingly, these patients can recover but have lingering deficits in the kinematic aspects of a prehension task (e.g., Roy et al. 2004), a function ascribed to area 5L (see Kalaska 1996).

Although posterior parietal cortex, including area 5, has been clearly implicated in complex manual and visuomanual behavior, the extent and gross topographic organization of this region has yet to be fully characterized, as has been done in multiunit mapping studies of somatosensory areas on the postcentral gyrus, in the central sulcus (CS), and in the lateral sulcus including areas 3a, 3b, 1, 2, S2, and PV (for review, see Krubitzer and Disbrow 2008). While neurons in this large area 5 zone respond best in awake and behaving animals, these types of preparations are not optimal for collecting data from a large extent of cortex where hundreds of densely spaced recording sites can be used to determine the extent and gross organization of a field in individual animals. Despite this problem, over the

Architectonic Divisions of the IPS

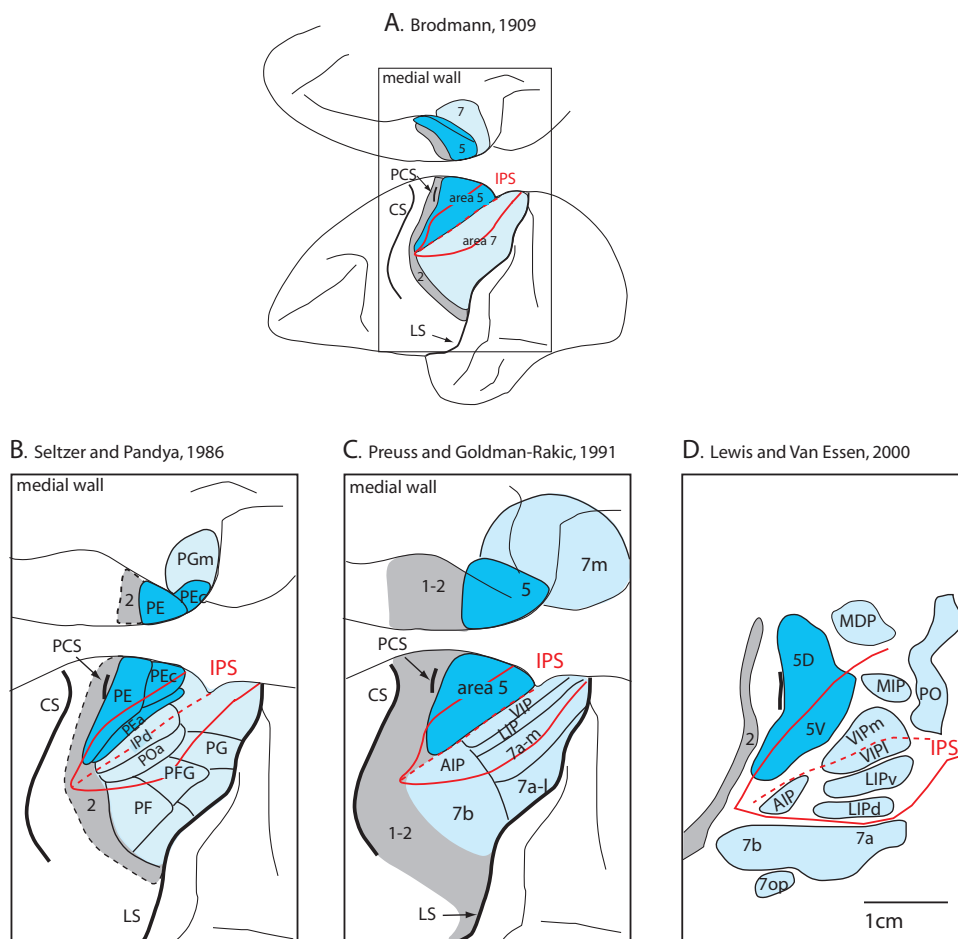


Figure 1. Architectonic parcellation of the IPS by different studies. The first scheme was proposed by Brodmann (A) and subsequent schemes with differing terminology were proposed by different investigators (B–D). In some modern parcellation schemes, BA5 has been subdivided into at least 2 fields. For abbreviations, see Table 1.

past decade, we took advantage of favorable conditions in anesthetized monkey experiments that formed parts of other studies in our laboratory to examine the receptive field characteristics and topographic organization of lateral portions of BA5, which we term area 5L.

Our goals were to explore the rostral bank of the IPS to examine the representation of somatic receptors (mechanosensory and proprioceptors), to determine whether the representation is complete and includes all portions of the body, and to describe the degree to which the hand and forelimb are magnified in this field. Using multiunit recording techniques has allowed us to reconstruct comprehensive functional maps of cortical areas that include regions within the traditionally defined BA5 and the adjacent area 2.

Materials and Methods

Multiunit microelectrode recording techniques combined with architectonic analysis were used to identify the location, boundaries, and topographic organization of BA5. Seven adult macaque monkeys (*Macaca mulatta*) weighing 8.3–14.0 kg were used. All experimental protocols conformed to National Institutes of Health guidelines and were approved by the Animal Use and Care Administrative Advisory Committee of the University of California, Davis.

Surgical Procedures

Aseptic surgical techniques were used in all terminal electrophysiological experiments. Each animal was initially anesthetized with ketamine hydrochloride (10 mg/kg, IM), and once anesthetized, the animal was intubated and cannulated and a surgical level of anesthesia was maintained with the inhalation anesthetic, isoflurane (1.2–2.0%, in 1 L/min O₂). Fluid levels were maintained with a continuous drip of lactated Ringer's (LS) solution alternated with LS + 2.5% dextrose (10 mL/kg/min, IV). Once anesthetized, the skin was cut, the temporal muscle was retracted, and a craniotomy was performed over the anterior parietal cortex and the posterior frontal cortex, exposing the precentral and postcentral gyri as well as the CS and IPS. Figure 2K shows the location of the mapped areas in relation to the CS and IPS. Next, a well was built around the skull opening and filled with silicon fluid (Dow Corning 200 fluid (dimethylpolysiloxane); Dow Corning, Midland, MI) to maintain cortical temperature and prevent desiccation. Throughout the recording experiment, heart rate, body temperature, blood oxygenation levels, and fluid levels were monitored and maintained and in one case (01–45), the animal was ventilated.

Electrophysiological Recordings

A digital image of the exposed cortex was taken with a Pixera PVC100C digital camera (Pixera, Los Gatos, CA) or CoolPix 5700 (Nikon, Melville, NY) so that electrode penetration sites, lesions, and probes could be related to blood vessel patterns. The recording electrode (low-impedance tungsten-in-varnish microelectrodes, 5 MΩ at 100 Hz;

Table 1

List of abbreviations

Cortical areas	
3b	Primary somatosensory area (S1; anterior parietal cortex)
1	Cutaneous representation caudal to 3b (anterior parietal cortex)
2	Representation of deep receptors caudal to area 1 (anterior parietal cortex)
5 (BA5)	Posterior parietal area 5 (Brodmann's area 5)
5d	Dorsal subdivision of posterior parietal area 5 (on the rostral SPL)
5v	Ventral subdivision of posterior parietal area 5 (in rostral bank of the IPS)
5L	Lateral division of area 5.
7	Posterior parietal area in caudal bank of IPS—contains several subdivisions
AIP	Anterior intraparietal area
CIP	Caudal intraparietal area
IPd	Intraparietal area (in depth of IPS, adjacent to POa and PEa)
LIP	Lateral intraparietal area
LIPd	Lateral intraparietal area (dorsal division)
LIPv	lateral intraparietal area (ventral division)
MIP	Medial intraparietal area
MIP	Medial intraparietal area (posterior parietal cortex)
PIP	Posterior intraparietal area
PE	Superior parietal lobule area
PEa	Superior parietal lobule area (anterior portion, in upper bank of IPS)
PEc	Superior parietal lobule area (caudal portion)
PF	Rostral inferior parietal lobule area
PFg	Rostral inferior parietal lobule area (transitional area between PF and PG)
PG	Rostral inferior parietal lobule area
PGm	Rostral inferior parietal lobule area (medial portion)
PO	Parietal occipital area (V6+V6a)
POa	Parietal occipital area (anterior portion)
PRR	Parietal reach region (posterior parietal cortex)
SPL	Superior parietal lobule
VIPd	Ventral intraparietal area (dorsal division)
VIPi	Ventral intraparietal area (lateral division)
VIPm	Ventral intraparietal area (medial division)
VIPv	Ventral intraparietal area (ventral division)
V6	Posterior parietal area of the IPS
V6A	Dorsal portion of area V6
Sulci	
CS	Central sulcus
IPS	Intraparietal sulcus
LS	Lateral sulcus
PCS	Postcentral sulcus
Body parts	
cn	Chin
D	Digit (individual)
d; di	Digits
el	Elbow
fa	Forearm
fl	Forelimb
ft	Foot
h; ha	Hand
hl	Hindlimb
htp	Hypothenar pad
kn	Knuckle
tr	Trunk
occ	Occiput
pr fl	Proximal forelimb
P/p	Pads
sh	Shoulder
sn	Snout
tp	Thenar pad
tr	Trunk
ul	Upper lip
vis	Visual
wr	Wrist
Anatomical directions	
dis; dist	Distal
dor	Dorsal
low	Lower
mid	Middle
r	Rostral

30 μm tip diameter) was placed perpendicular to the cortical surface and a hydraulic microdrive (Kopf Instruments, Tujunga, CA) was used to lower the electrode into the cortex, including the depths of the CS and IPS. The neural response was amplified, filtered, and monitored through a loudspeaker and on an oscilloscope. For recordings on the surface of cortex, electrodes were lowered 700–1000 μm below the pial surface. For recordings in the sulci, the electrode was positioned so

that it ran parallel to the pial surface through layer IV and was advanced in increments of 500 μm . Once the electrode was in place, the body surface was stimulated and the receptive fields for neurons at that cortical site were drawn on diagrams of the monkey's body.

Cutaneous stimulation consisted of light displacements of the skin with a fine probe and light brushing of hairs and skin. Light to moderate taps, digit and limb manipulation, and light pressure, categorized as “deep stimulation,” were used to stimulate the muscles, joints, and skin. In all animals, the contralateral and ipsilateral body surface, joints, and musculature were stimulated. Full field flashes of light were used to determine if neurons responded to visual stimulation. Selected recording sites in these experiments were marked by coating the recording electrode with a 10% solution of diamidino yellow (DY; Sigma, St Louis, MO) and then reinserting the electrode into the cortex at sites either on the surface of the cortex or into the depths of the CS or IPS. This method allowed us to readily identify selected electrode penetrations, determine electrode angle for the penetrations into the banks of sulci, and relate recording sites to histologically processed tissue (see Padberg et al. 2009).

Histological Processing

Following the completion of the recording experiment, the monkey was transcardially perfused with 0.9% saline in 0.1 M phosphate buffer (PB), followed by 4% paraformaldehyde in PB (pH 7.4), and then 4% paraformaldehyde in 10% sucrose PB. The brain was then extracted and postfixed in 30% sucrose PB overnight. In 4 cases, the brain was left intact and sectioned horizontally so that laminar distinctions of cortical fields could be appreciated. In the remaining 3 cases, the corpus callosum was transected and the cortex was peeled away from the basal ganglia and diencephalon; sulci were gently opened and the gyri flattened. The entire cerebral hemisphere was flattened between a lightly weighted glass slide and a large glass Petri dish filled with 4% paraformaldehyde in 30% sucrose PB. These cortices were then sectioned tangentially.

After fixation and cryoprotection, flattened cortices and whole brains were frozen on a sliding microtome stage. Flattened cortices were sliced tangential to the pial surface into 50- μm sections, and whole brains were sliced in the horizontal plane into 60- to 80- μm sections. For the horizontally sectioned tissue, alternate sections were stained for Nissl substance (Fig. 3*B–D*) or cytochrome oxidase reactivity (Carroll and Wong-Riley 1984). Flattened cortices were stained for myelin using the Gallyas (1979) method to reveal cortical architecture (Fig. 3*E,F*).

Data Analysis

Functional electrophysiological maps of the brain were generated by analyzing receptive field positions and stimulus preferences at all sites and drawing interpolated boundaries between different body part representations. Recording sites that had neurons with the same receptive field were grouped together and lines were drawn between these recording sites and those that had neurons with different receptive fields. In some instances, if 1 or 2 unresponsive sites fell within a larger zone of responsive sites with similar receptive fields, they were incorporated within this larger zone and marked with an X to keep the maps from getting too congested.

The angle of our electrode penetrations on the banks of the CS and IPS was determined from electrode tracks and the DY probes on Nissl-stained and/or myelin-stained sections (Fig. 3*E,F*, arrows). We next determined the architectonic boundaries of areas 3b, 1, 2, and the lateral and middle portion of BA5. In flattened cortical tissue stained for myelin, architectonic boundaries were drawn based on the density of myelination. The entire series of sections was used to determine cortical boundaries since most often all cortical field boundaries could not be determined from a single section. In addition, the outline of the section, blood vessels, tissue artifacts, fiducial probes, and electrode angles were also drawn. By aligning these landmarks, architectonic boundaries throughout the entire depth of the cortex were obtained. This architectonic reconstruction was directly related to the electrophysiological recordings by aligning the probes drawn on the picture of the brain with those found in the histologically processed tissue. In this

Electrophysiological Recordings in “area 5” in the IPS

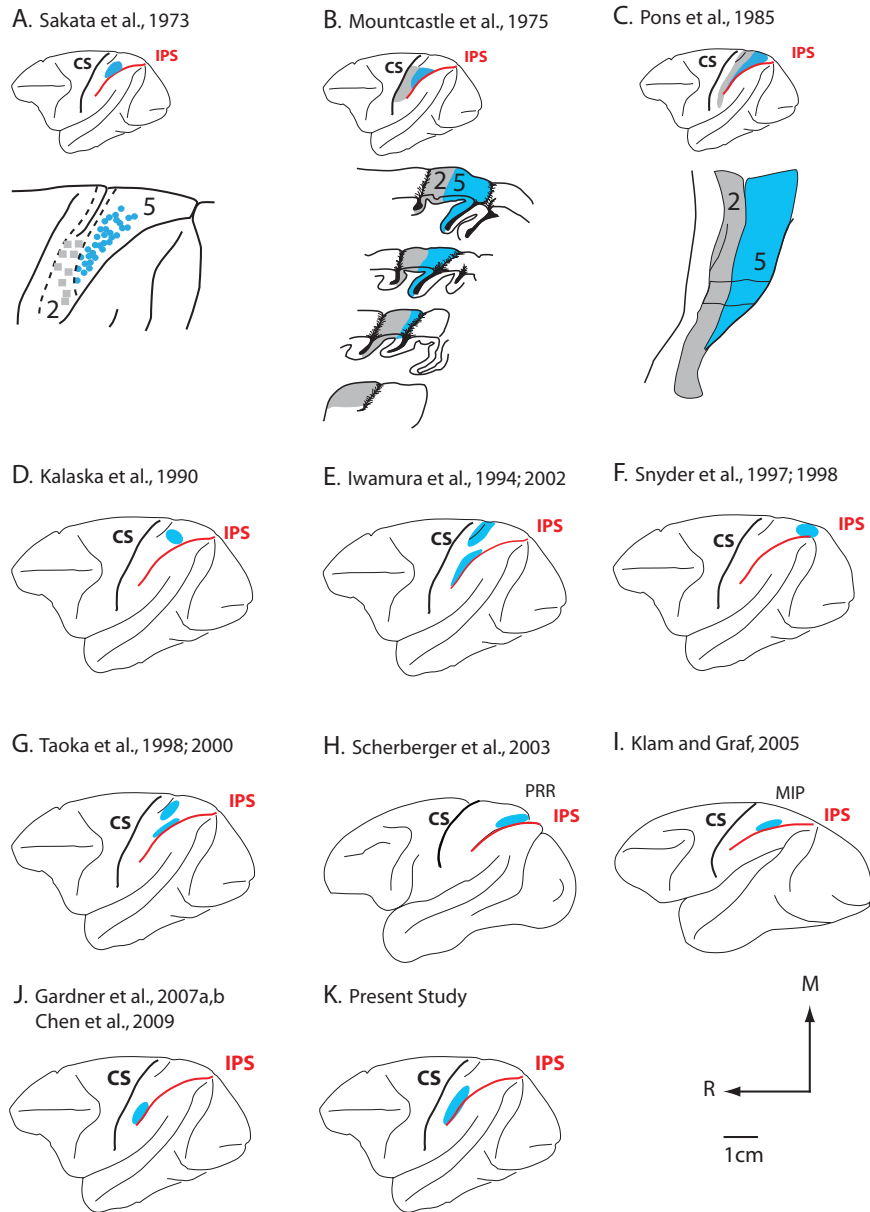


Figure 2. The location of recording sites in different portions of BA5 in different studies. Some studies were in a middle portion of BA5 (A–C,G,I), some studies recorded from medial portion of BA5 (D–F,H), and some studies recorded from lateral portion of area 5 (E,G,J,K). These recording sites do not always correspond to architectonic subdivisions within BA5. The arrows indicate anatomic directions, and the scale bar is for D–K. Conventions as in previous figure.

way, a single comprehensive reconstruction of the architectonic boundaries relative to the electrophysiological recording sites was made. In the horizontally sectioned tissue, we used a camera lucida to draw architectonic boundaries from the series of tissue stained for myelin and Nissl. These drawings included the outline of the section, blood vessels, tissue artifacts, fiducial probes, and electrode tracks. By aligning the series of sections using the fiducial probes, a cortical surface reconstruction could be made and aligned with the photograph of electrode penetrations. As before, this allowed us to produce a comprehensive reconstruction that included architectonic boundaries, sulcal landmarks, surface electrode penetrations, and the entire extent and angle of electrode penetrations made into the CS and IPS. Digital images were made with a Nikon Copy Camera (Tokyo, Japan) with a Phase One PowerPhase FX+ (Global Manufacturing, Louisville, CO) digital back. The digital image was taken using PowerPhase FX

Image Capture software (Global Manufacturing, Louisville, CO). The image was cropped and put into grayscale using Adobe Photoshop (Adobe Systems Incorporated, San Jose, CA). Final drawings and digital images were generated and assembled using Adobe Photoshop and Illustrator software packages (Adobe Systems Incorporated, San Jose, CA). Measurements of area 5L were made using the debugger palette in Adobe Illustrator CS2. MIP was not included in our measurements.

The total number of recording sites was determined for each cortical field in each animal and the proportion of recording sites in which neurons responded to a particular submodality (i.e., responsive to cutaneous stimuli, responsive to deep stimuli) was calculated using analysis of variance (Excel, Microsoft, Redmond, WA). Planned comparisons (2-sample t-tests assuming equal variances) were then performed to assess differences between cortical fields. For all analyses, $\alpha < 0.05$.

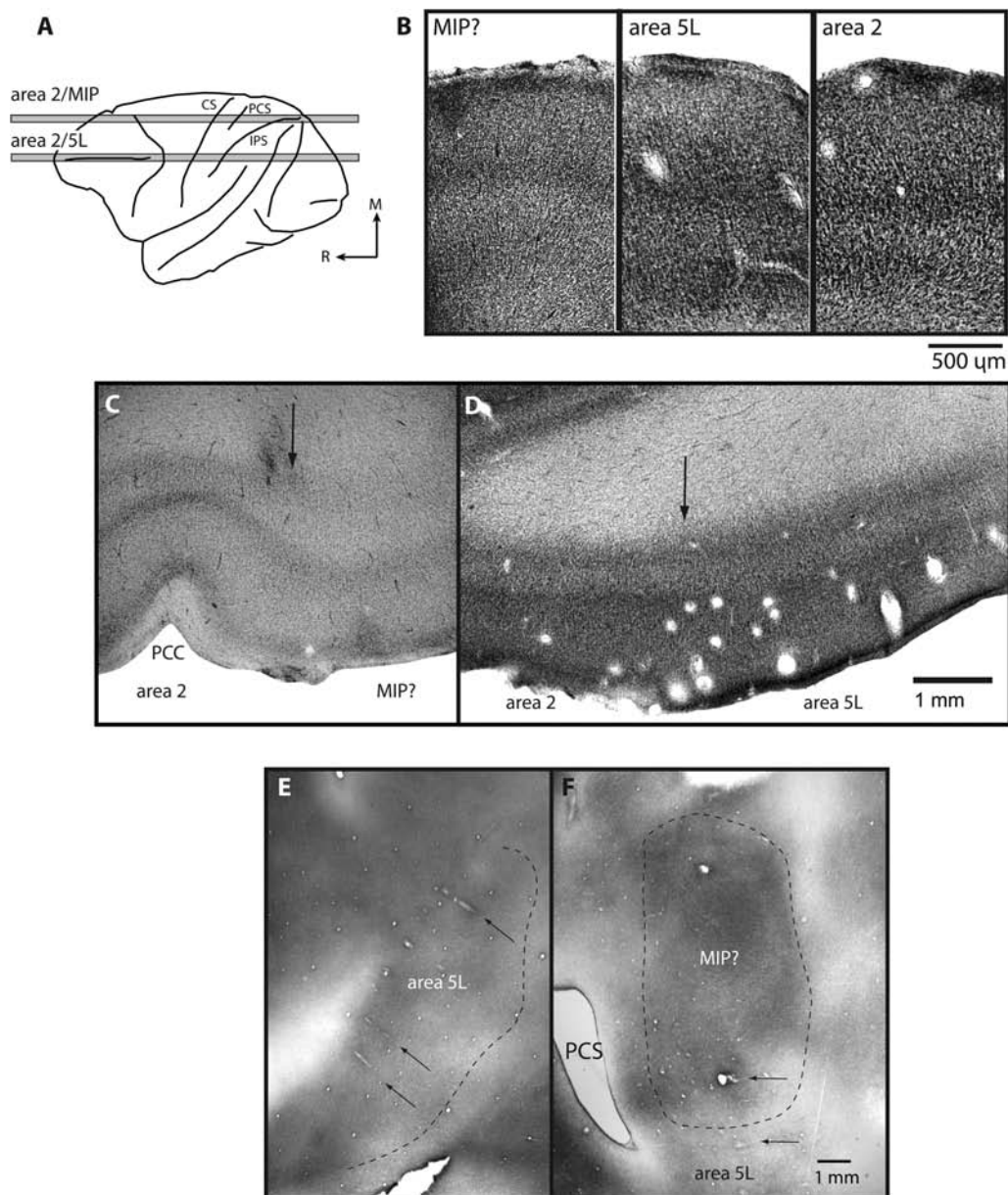


Figure 3. A dorsolateral drawing of the brain (A) showing the locations from which sections B–D were taken (gray bars). (B) High-powered images of cortex sectioned horizontally and stained for Nissl allow for a direct comparison of the laminar organization of areas 2, area 5L, and the presumptive area MIP. (C) The area 2 and presumptive MIP border are characterized by a dramatic decrease in cell density of layers IV and VI in MIP? as well as a thickening of these layers. (D) The area 2/5L boundary is characterized by a slight decrease in density and a thickening of layers IV and VI. These differences are not as distinct as those between the borders of area 2 and MIP?. In the flattened preparations that have been stained for myelin (E and F) some of the borders of areas 5L and MIP are visible. However, the entire series of sections is used to determine all of the boundaries of these fields. This type of preparation allows much of the length of individual recording tracks within the IPS to be readily appreciated (black arrows). Cortical field boundaries are marked by an arrow in C and D and with a dashed line in E and F. Photomicrographs were taken from cases 01-45 (F); 03-141 (D); 04-51 (B: area 2); 04-53 (B: MIP? and C); 05-82 (E); 05-116 (B: area 5L). Conventions as in previous figures.

Results

Multiunit electrophysiological recordings were made at multiple densely spaced (500 μm apart) sites in and around the IPS (Figs 5 and 6) in each of 6 macaque monkeys so that the overall topographic organization of area 5L, and the adjacent hand representation of area 2, could be determined and directly related to histologically processed tissue. In one additional case, recordings were made in cortex medial to area 5L in the IPS. In the following results, we first describe the cyto- and myeloarchitectonic appearance of areas 2, 5L, and the medial IPS region in both horizontally and tangentially sectioned

neocortex, respectively. We then describe electrophysiological recording and the organization of receptive fields in areas 2, 5L, and the medial IPS region.

Cyto- and Myeloarchitecture of Areas 2, 5L, and the Medial IPS Region

In 3 cases, cortex was flattened and cut parallel to the pial surface and in 4 cases, the cortex was sectioned horizontally. Myelin staining in flattened cortex allowed us to appreciate the entire extent of each field and the spatial relationship of each field to other fields as well as the angle of our recording

electrodes into the sulci (Fig. 3E,F, black arrows). In this preparation, area 5L can be readily observed as a moderately myelinated field in the rostral bank of the IPS. In cortex that was horizontally sectioned and stained for Nissl substance, area 5L can be distinguished by relatively thick and moderately staining layers IV and VI (Fig. 3B,D). Area 5L's ventral boundary in the depths of the IPS is distinguished from the neighboring regions of cortex by a thinning of these 2 layers. Its boundary with area 2 is less distinct since in area 2 layers IV and VI are also thick and darkly staining. However, in area 2, these layers are slightly more dense and somewhat thinner than in area 5L. In area 2, layers IV and VI are more darkly staining and somewhat thicker than similar layers in the rostrally adjacent area 1 (also see Pons et al. 1985b). In tangentially sectioned tissue stained for myelin, area 2 is moderately myelinated compared with the more darkly myelinated area 1 located rostrally. Because area 5L is also moderately myelinated, it is sometimes difficult to distinguish the area 2/5L border in this preparation. The myelo- and cytoarchitecture of anterior parietal areas 3a and 3b have been well described in macaque monkeys in previous studies in our own laboratory (Krubitzer et al. 2004) and other laboratories (e.g., Nelson et al. 1980; Darian-Smith and Darian-Smith 1993). Using combined architectonic data and electrophysiological recordings the boundaries of area 5L were drawn and its areal extent was measured. The measurements revealed that area 5L has a mean area of 50.6 mm² (standard deviation = 9.9 mm²).

Cortex just medial to area 5 was architectonically distinct from both areas 2 and 5. This region which we term the presumptive area MIP (MIP?) differed from the rostrally located area 2 by a decrease in density in layers IV and VI (especially layer VI) and a thickening of these layers (Fig. 3B,C). Its cytoarchitectonic appearance differed from area 5L by a decrease in cell density and broadening of layer VI. In cortex flattened and stained for myelin, this medial IPS region could be seen as a moderately myelinated field compared with area 2 and was slightly more densely myelinated than area 5 (Fig. 3F).

Electrophysiological Recording Results

In all cases, multiple recording sites were made in the caudal bank of the CS on the postcentral gyrus and in the rostral bank of the IPS (see Supplementary Fig s1 and 2). Table 2 provides the overall number of responsive and unresponsive recording sites in areas 2 and 5L for each case. Our overall goal was to examine the complete organization of area 5L. To accomplish this, we distinguished area 5L from surrounding cortical areas using both architectonic analysis (see above) and functional criteria. Thus, cortex adjacent to the rostral, lateral, caudal, and medial borders of area 5L were also examined when possible. Area 2 is located rostrally to area 5L and complete maps of this area have been generated in previous studies (e.g., Pons et al. 1985b). Thus, we did not attempt to explore area 2 in its entirety but recorded only from the portions of area 2 that were adjacent to area 5L, which includes the hand representation, a small part of the face representation, and a part of the forelimb representation. In the following sections, we describe several outstanding features of our results.

Submodality of Response in Areas 2 and 5L

Cortical area 2 is located on the caudal half of the postcentral gyrus and cortical area 5L is located mostly within the rostral

Table 2
Number and distribution of recording sites

Case	Area 2		Area 5L		Total sites
	R	UR	R	UR	
03-117	49	6	28	37	120
03-141	50	6	90	31	177
04-51	45	3	61	16	125
05-82	56	0	75	11	142
05-116	56	16	40	21	133
07-64	53	5	24	32	114
Total	309	36	318	148	811

Case	Area 2		MIP?		Total sites
	R	UR	R	UR	
01-45	30	1	67	25	123

Note: R, responsive sites; UR, unresponsive sites.

bank of the lateral IPS. Although area 5 neurons respond maximally when the animal is awake rather than anesthetized (Mountcastle et al. 1975), in most cases, we were able to drive neurons while using isoflurane anesthesia. However, in these experiments relatively more sites in area 5 were unresponsive to any form of stimulation than in area 2 (see Table 2).

The submodality of response, that is whether neurons responded to cutaneous or noncutaneous stimulation, changed significantly across the areas examined in this study (cutaneous responses: $F_{3,19} = 44.3$, $P < 0.0001$; noncutaneous responses: $F_{3,19} = 48.2$, $P < 0.0001$). Furthermore, neurons in area 5L responded significantly more to stimulation of muscles and joints than neurons in area 3b, 1, and 2 ($t_0 = -10.9$, $P < 0.0001$; $t_{10} = -16.3$, $P < 0.0001$; $t_{10} = -3.4$, $P < 0.005$, respectively). Likewise, neurons in area 5L responded significantly less to cutaneous stimulation than neurons in area 3b, 1, and 2 ($t_0 = 9.9$, $P < 0.0001$; $t_{10} = 14.0$, $P < 0.0001$; $t_{10} = 3.2$, $P < 0.05$, respectively). In area 5L, 90% of the sites that responded to sensory stimulation contained neurons that responded to joint manipulation and muscle palpation (Figs 4-6) and 10% of the sites contained neurons that responded to cutaneous stimulation and these differences were significant. About 4% of the recording sites also contained neurons that responded to visual stimulation and neurons in 2% of the sites had bilateral receptive fields.

In area 2, the proportionality of response changed dramatically with 58% of responsive recording sites containing neurons that respond to joint manipulation, muscle palpation, and taps to a body part and 42% of the responsive sites containing neurons that responded to cutaneous stimulation. Neurons in area 2 responded significantly less to cutaneous stimulation than neurons within area 3b ($t_{10} = 4.5$, $P < 0.001$) and area 1 ($t_{10} = 5.8$, $P < 0.001$) but significantly more than neurons in area 5L ($t_{10} = 3.2$, $P < 0.05$). Likewise, neurons in area 2 responded significantly more to stimulation of joints and muscles than neurons within area 3b ($t_{10} = 4.5$, $P < 0.001$) and area 1 ($t_{10} = 16.3$, $P < 0.0001$) but significantly less than neurons in area 5L ($t_{10} = -3.4$, $P < 0.005$) (Fig. 4). However, the responses of neurons in area 2 to cutaneous and deep stimulation did not significantly differ ($t_{10} = -1.4$, $P = 0.09$). About 2% of neurons in area 2 responded to visual stimulation, while none of the sites contained neurons with bilateral receptive fields.

The organization of areas 3b and 1 has been well documented in a number of New and Old World monkeys

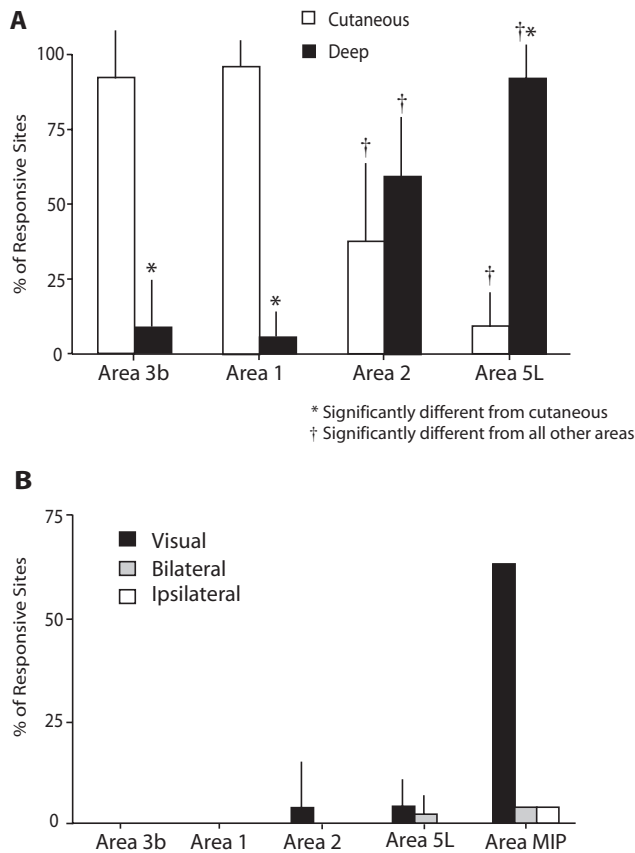


Figure 4. Histograms depicting the percentage of recording sites in which neurons in anterior and posterior parietal areas responded to (A) cutaneous versus deep stimulation or (B) visual, bilateral, or ipsilateral stimulation. The submodality to which neurons respond is distinct across cortical areas. The responsiveness of neurons to visual stimulation in area MIP is one of the distinguishing features of this field. Mean \pm standard deviation, $P < 0.05$. *—significantly different from cutaneous. †—significantly different from all other areas.

(for review, see Krubitzer and Disbrow 2008) and will not be described in detail here. However, a feature that distinguished these areas from areas 2 and 5L was the proportion of neurons that responded to cutaneous stimulation. As in previous studies, we observed that the vast majority of neurons on the caudal bank of the CS (91%) and on the rostral portion of the postcentral gyrus (95%) preferentially responded to cutaneous stimulation over deep stimulation (Fig. 4). Neither area 3b nor 1 contained neurons that had bilateral receptive fields or responded to visual stimulation.

Topographic Organization and Receptive Field Configuration of Areas 2 and 5L

The topographic organization of area 2 has been previously described in macaque monkeys (e.g., Pons et al. 1985a, 1985b; Padberg et al. 2010) and our results are similar to these previous studies (Figs 5 and 6). Figures 5 and 6 show detailed reconstructions of the cortical maps in areas 5L and 2 and Figure 7 shows receptive fields for selected recording sites in area 5L. In all cases, even those in which fewer recording sites were obtained within area 2, the forelimb, hand, and face were represented in an orderly fashion from medial to lateral. Within the hand representation, digit 1 was represented in the most lateral location, digit 2 was represented medial to this, and digits

3–5 were often represented in various combinations medial to the D2 representation. The location of the representation of the pads varied and was sometimes located rostral to the digit representations (e.g., Fig. 5B,C) and sometimes located both rostral and caudal to the digit representations (e.g., Fig. 5A). Finally, the representation of the dorsal hand and digits were found in islands within the digit representation (Figs 5C and 6C). We observed relatively contiguous representations of major hand or digit parts, and re-representation of the same body part in area 2 were rare. Our partial maps of area 2 are very similar to the full maps generated by Pons et al. (1985a, 1985b) in that the pad representation was in variable locations in different cases, and there was often a grouping together of digits 3–5, rather than single digit representation as in areas 3b and 1 (for review, see Fig. 9).

It was more difficult to generate maps for area 5L for 4 reasons. The first is that in several cases, we could not elicit responses from neurons at all sites in area 5L (Table 2). Second, similar body parts were often represented multiple times in noncontiguous locations. However, we were able to establish a general topographic order for area 5L with the proximal forelimb represented medially and the hand and digits represented more laterally (Figs 5 and 6). The third is that multiple hand parts were often represented at a single site so that drawing lines that interpolated different hand parts was not as straight forward as for area 2. For example, rather than encompassing 1 or 2 digits or a small portion of the palm, receptive fields for neurons in area 5L often encompassed multiple digits, digits plus the palm or a larger portion of the palm. Also, receptive fields were sometimes located on 2 or 3 different body parts like the knuckles, elbow, and shoulder (e.g., Fig. 7A). Finally, compared with area 2, in area 5L, the representations of the different parts of the forelimb were more variable (compare maps in Figs 5 and 6). While the presence of some unresponsive pockets could contribute to the disorderly representation in area 5L it is unlikely that this would explain a fractured organization in all cases, since several of the cases (e.g., Fig. 5A,C and Table 2) had relatively few unresponsive regions and the maps in these cases were still fractured.

Neurons in area 5L responded predominantly to stimulation of muscles and joints, and representations of cutaneous receptors were only noted in a small number of sites in a few cases (Fig. 4A, open circles in Figs 5B and 6A,B). Most neurons in area 5L had receptive fields on the contralateral side of the body, but bilateral receptive fields were identified in 3 cases (Figs 5A,B and 6C, gray squares; Fig. 7B, receptive fields a and b). Finally, responses to visual stimulation were observed at a few sites in 3 cases (Figs 5A,B and 6C, gray circles). In many instances, flexing the digits, knuckles and/or wrist, or rotating a joint elicited a good response, compared with taps, as in area 2. Furthermore, in several instances, movement of the knuckles, wrist, and elbow elicited a neuronal response within a single recording site (e.g., Figs 5A, 6C, and 7). The most striking feature of area 5L was the magnification of the forelimb and hand and apparent lack of any other body part representation (for summary, see Fig. 9).

Although a clear reversal in receptive field progression was not observed across the area 2/5L boundary, there were several features of representation and receptive field size and configuration that helped distinguish area 5L from area 2 (illustrated in Figs 4–6). For example, we compared the spatial

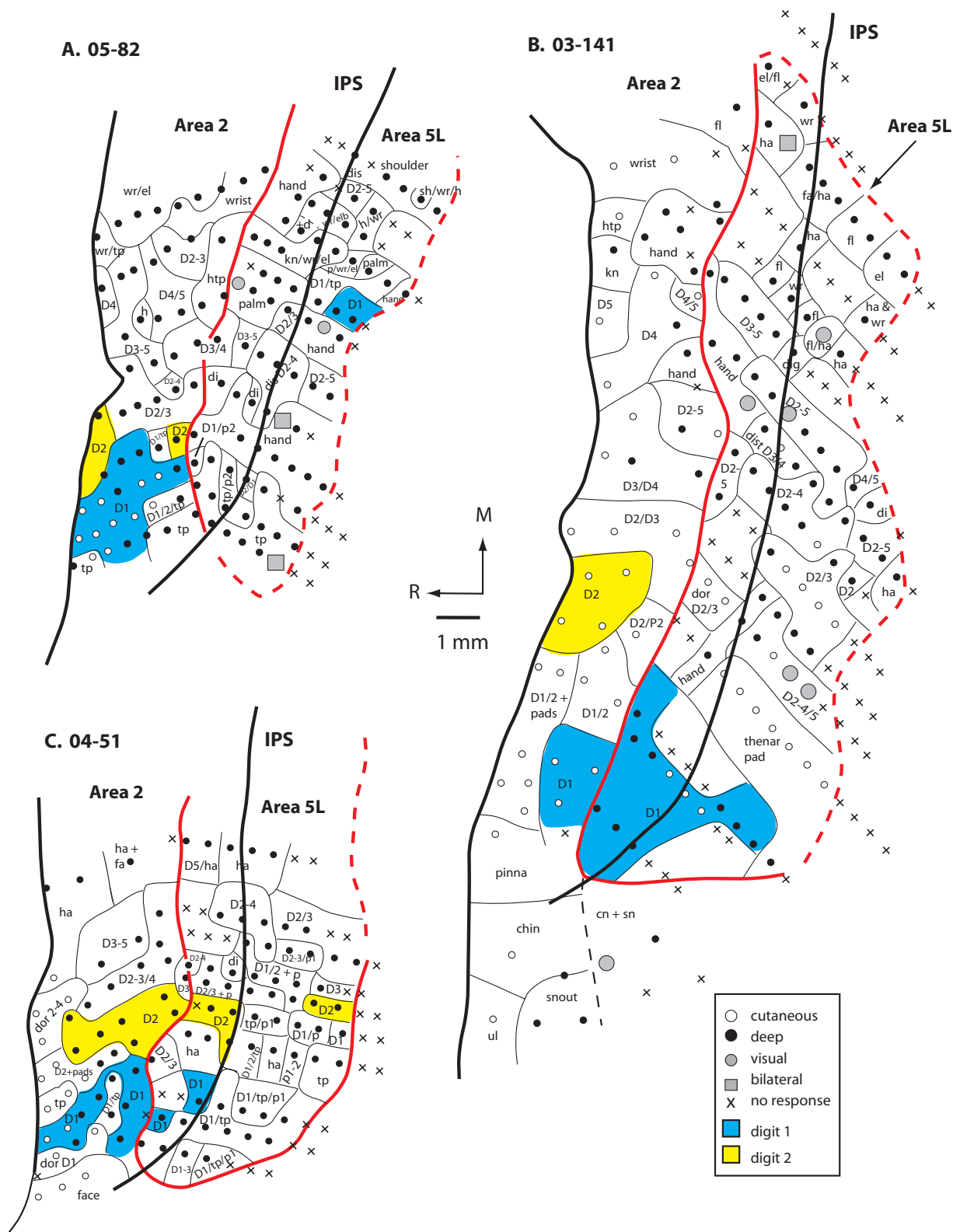


Figure 5. Maps of area 5L and portions of area 2 generated from electrophysiological recordings in the 3 cases (A. 05-82, B. 03-141, and C. 04-51). In these cases, most of the neurons in area 5 were responsive to stimulation of deep receptors of the skin, muscle, and joints (closed circles). In 2 cases, there were a few sites in which neurons responded to visual stimulation (A and B; gray circles) and in 2 cases, neurons had bilateral receptive fields (A and B; gray squares). The topographic organization of area 2 could be readily discerned, but in area 5L, the same body part was represented multiple times and was encompassed in different receptive field configurations. Furthermore, only the forelimb, and not the head or trunk, was represented in area 5L. Also, there was a greater degree of variability in map organization between individual cases in area 5L compared with area 2. The representations of digits 1 (blue) and 2 (yellow) are highlighted so that direct comparisons can be made between areas 2 and 5L. Area 2 has distinct individual representation of both D1 and D2 while this is variable in area 5L. Most often these digits are represented with other digits rather than individually in area 5L. Thick solid and dashed lines indicate architectonic borders and thin lines separate different body part representation with each cortical area. The red outlines area 5L. The IPS is denoted as a thick black line that runs through area 5L in the mediolateral plane. Other conventions as in previous figures.

Receptive fields for neurons in area 5L

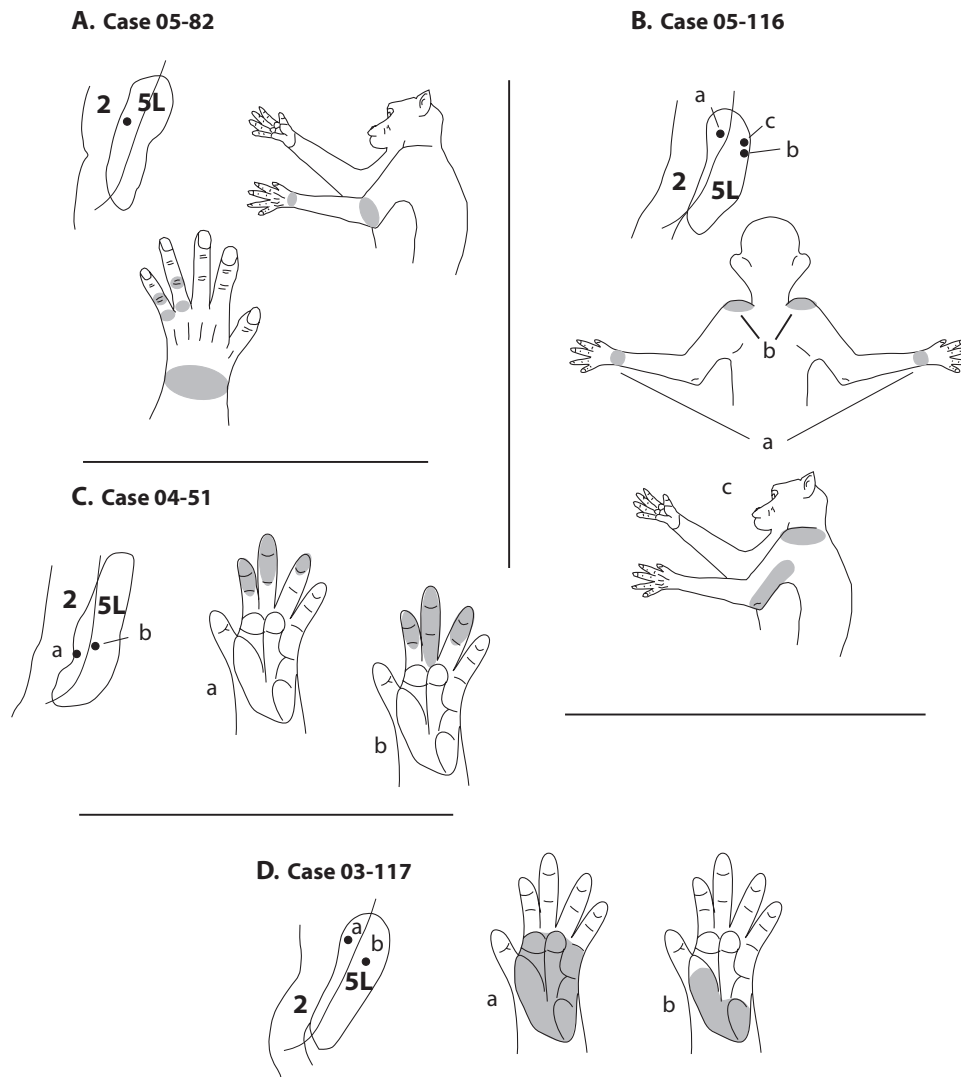


Figure 7. Examples of receptive field composition for neurons in area 5L from 4 cases (A–D). These examples demonstrate that receptive fields were complex and often involved several different portions of the forelimb such as the knuckles, wrist, and elbow (A) or elbow and shoulder (B; bottom figure). In some cases, neurons had bilateral receptive fields (B; top figure). Multiple digits were often encompassed in a receptive field (C) or relatively large portions of the palm were represented (D). Neurons at all of these sites responded to manipulation of the joints and muscles or taps to portions of the skin. The small insets below each case number illustrate portions of area 2 and area 5L and the location of the recording sites within area 5L that correspond to the receptive fields drawn for each case.

extent of body part representations that incorporated the same body parts (Figs 5 and 6, yellow and blue regions). In area 2, there is a single contiguous representation of D1 and D2 (with one exception), while digits 3–5 are often (but not always represented together in various combinations). In area 5L, the individual representations of D1 were observed once or twice in various locations and in one case, D2 was represented in 2 locations. Most often these digits were represented multiple times at noncontinuous locations, with neurons in each of these locations having receptive fields on the same body part and often other body parts. These multiple representations of a body part, often conjoined with other limb or hand representations, and produced a fractured map in area 5L, much like that reported for motor cortex (e.g., Gould et al. 1986; Stepniewska et al. 1993; Wu et al. 2000; Remple et al. 2006).

Cortex Medial to Area 5L

In one case, we explored the medial portion of the rostral bank of the IPS (Fig. 8). This region was bordered rostrally by the shoulder, trunk, and hindlimb representation in area 2 and neurons in this medial IPS region were responsive to stimulation of skin, muscle, and joints. While most of the receptive fields for neurons in this region were on the contralateral body, 8% of recording sites had neurons with receptive fields on the ipsilateral body and/or bilateral receptive fields. Furthermore, unlike areas 2 and 5L, 63% of the sites contained neurons responsive to visual stimulation either alone or in combination with somatic stimulation (Fig. 4B). Although the representation of the body was fractured and there were sites in which neurons were unresponsive to any type of stimulation, there was a general topography in this region with the hindlimb represented far

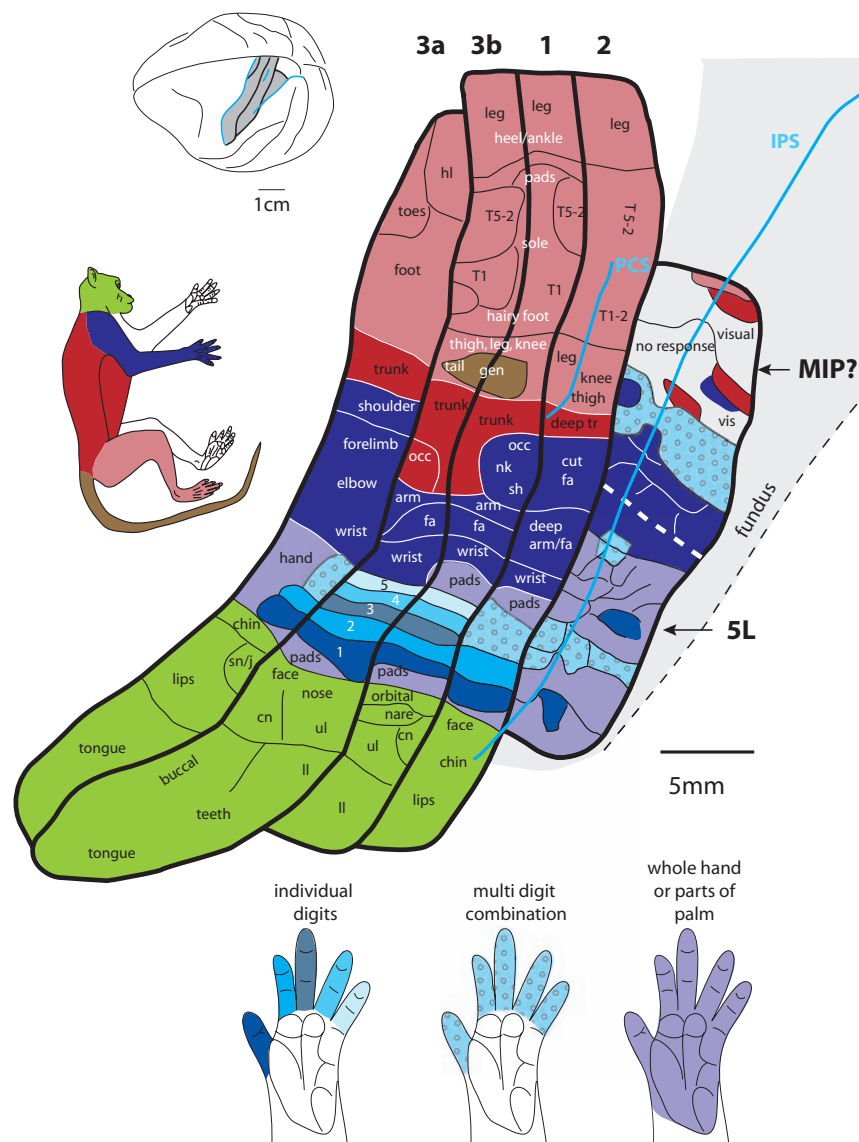


Figure 9. A summary of the functional subdivisions of anterior parietal areas 3a, 3b, 1, and 2 and posterior parietal areas 5L and the presumptive MIP. While anterior parietal areas have a clear parallel mediolateral organization, this type of organization is not observed in posterior parietal areas. Both MIP? and area 5L have fractured maps that are dominated by representations of the digits, hand, and forelimb. The solid gray corresponds to BA5 and area 5L and the presumptive MIP depicted here fall within this larger zone. Noted that in areas 3b and 1, all digits are represented individually, while in areas 3a and 2, only digits 1 and 2 are represented individually; digits 3–5 are generally represented together. In area 5L, sometimes digit 1 or 2 is represented individually, but most often multiple digits are represented in different combinations (light blue stipple) or parts of the hand or the whole hand is represented (light purple). General topographic organization of areas 3a, 3b, 1, and 2 are redrawn from data from the current study and that of Krubitzer et al. (2004), Nelson et al. (1980), and Pons et al. (1985b), respectively; the genital/tail representation in areas 3b and 1 is from Rothmund et al. (2002). Conventions as in previous figures.

Compared with that of area 2 or anterior parietal areas 3b and 1, in area 5L, there were more individual differences across cases in terms of location, contiguity, and relative size of different hand part representations.

Although there is only one case in which the anesthetic level was favorable and allowed us to record from neurons in a location medial to area 5L, the location, functional organization, architecture, and neural properties of this field indicate that it may be different than area 5L, and previous single unit electrophysiological recording studies indicate that it is a separate field (see Discussion). This medial region contains small hindlimb and trunk representations and a larger representation of portions of the forelimb. Also, many neurons in this

region are responsive to visual stimulation and there are often islands of neurons that only respond to visual stimulation.

Discussion

This study provides the first full description of the topographic organization of the lateral portion of the IPS, traditionally incorporated in the larger architectonically defined area 5, and distinguishes the laterally located 5L from more medial locations that have been previously described (e.g., MIP; Colby and Duhamel 1991, 1996). Furthermore, this is the first demonstration of a large magnification of the forelimb and hand for any parietal area, with no apparent representation of other body

parts. Thus, the rules for simple topographic mapping of the entire contralateral sensory epithelium as seen in anterior parietal fields are not observed in areas of posterior parietal cortex, suggesting that other organizational principles are involved in functional map construction in these areas (Fig. 9). Finally, we demonstrate that the maps in area 5L + the presumptive MIP are not strictly topographic but fractured, more like motor cortical areas than the simple maps of the body in early stages of somatosensory processing in anterior parietal fields.

The methods for subdividing different regions of the neocortex have been described previously (e.g., Kaas 1982; Krubitzer 2009). Several criteria are used to subdivide a cortical field including topographic organization, neural response properties, stimulus preferences, architectonic appearance, and neuroanatomical connections. Posterior parietal areas have also been subdivided based on the various actions that they are associated with. While each criterion is important, when used in isolation it may not be sufficient to distinguish a field. For example, the use of single unit recordings alone to examine neural response properties without the use of cortical architecture or other criteria may not distinguish one field from another if the adjacent field has similar or overlapping neural characteristics. Furthermore, the use of cortical architecture alone can be misleading since different functional fields may have a similar architectonic appearance, and often similar architectonic methods generate different results in different laboratories (e.g., Fig. 1). Thus, the use of multiple criteria such as electrophysiological results in conjunction with cortical architecture and neuroanatomical connections are usually the best way to distinguish cortical fields.

In the current investigation, we used multiunit recording techniques combined with cortical architecture to distinguish area 2 from area 5L. Previous studies in our own and other laboratories demonstrate that the thalamocortical and cortico-cortical connections of area 5L versus area 2 are distinct as well (see Padberg et al. 2009). While the architectonic and functional distinction between area 2 and more medial portions of BA 5 (such as the presumptive MIP) are clear, the functional distinction between area 5L and the presumptive MIP are less distinct.

Although we consider these as separate fields, there are several issues with subdividing areas of posterior parietal cortex that make it difficult to draw firm conclusions about these regions. First, as noted in the introduction, neurons in area 5 respond optimally in awake animals, and electrophysiological recording results are affected by the anesthetic state. Because of this, it is not surprising that in the current study 45% of the recording sites in the IPS contain neurons that are unresponsive to somatic or visual stimulation (Table 2). While the architectonic appearance of the medial and lateral portions of area 5 are distinct (Fig. 3B), the physiological distinctions between these fields are less clear. Thus, an alternate interpretation is that the medial and lateral portions of area 5 form one very large field that runs from the lateral tip of the IPS to more medial portions of the IPS, adjacent to the PCS. This larger area 5 would still possess a magnified representation of the forelimb with many fractures in organization and rerepresentations of similar hand and limb parts. Furthermore, this single field would still appear to possess only a very small representation of the hindlimb and trunk. One way to help resolve the issue of whether 1 or 2 fields exist would be to examine the cortical and thalamocortical connections of medial and lateral portions of the rostral bank of the IPS, with

the expectation that if these are in fact separate areas, they would have distinct patterns of connectivity. This study is currently being conducted in our laboratory.

Regardless of our interpretation, the difference between areas on the rostral bank of the IPS (5L + the presumptive MIP) and area 2 are quite clear (Fig. 9). Furthermore, the caudal bank of the IPS has been subdivided into multiple cortical areas including AIP, LIP, VIP, and CIP, each associated with specific actions such as grasping, saccade guidance, heading perception, and 3D surface orientation (for review, see Tsutsui et al. 2005; Britten 2008; Bisley and Goldberg 2010). Thus, the notion that the very large BA 5 may be broken into separate fields including an area 5L as well as more medial divisions is not surprising.

Location and Organization of Areas 2 and 5L in Macaque Monkeys

The full topographic organization and receptive field characteristics of neurons in area 2 have been described in detail for macaque monkeys (e.g., Hyvärinen and Poranen 1978; Pons et al. 1985a, 1985b; Taoka et al. 1998, 2000; for review, see Iwamura et al. 2002) and cebus monkeys (Padberg et al. 2007). As in anterior parietal fields 3a, 3b, and 1, area 2 has a parallel representation with the leg and foot represented medially, followed by the toes, hindlimb, and trunk representation just rostral and caudal to the PCS (Fig. 9). The shoulder, wrist, digits, and face are represented most laterally. Some neurons in area 2 respond to stimulation of cutaneous receptors but the majority of neurons respond to stimulation of deep tissue (67%; Taoka et al. 1998) or noncutaneous stimulation of varying types (57%; Hyvärinen and Poranen 1978). Previous studies also found that 11–17% of neurons in area 2 had bilateral and ipsilateral receptive fields (Taoka et al. 1998) with the highest proportion (68%) located on the trunk. In the present study, the general topographic representation, receptive field size and receptive field configurations are similar to those reported previously by Pons et al. (1985a, 1985b). Likewise, we found that the majority (58%) of neurons in area 2 responded to stimulation of deep receptors. Neurons at a few sites in area 2 responded to visual stimulation. Although we did not find bilateral receptive fields in area 2, this may be due to our anesthetized preparation where callosal inputs to area 2 (and to area 5L) may have been completely or partially inhibited. Our data for area 2 support previous data on the organization of area 2 and demonstrate that the functional boundary of area 2 matches the architectonically defined border with area 5.

Unlike the parallel organization of body representations found in anterior parietal fields, our recordings in IPS showed a very different nonparallel organization with most of our lateral and medial recordings sites containing neurons with receptive fields on portions of the forelimb. Even if one were to consider area 5L and the presumptive MIP as a single field, this fractured organization with a magnified forelimb is still distinct. In early electrophysiological recording studies in area 5 in awake monkeys (for location of recordings, See Fig. 2), Duffy and Burchfield (1971), Sakata et al. (1973), and Mountcastle et al. (1975) (see Fig. 2A,B) report that receptive fields for neurons in area 5 were larger than in S1 and that most neurons (66–84%) responded to passive stimulation of deep tissue and joint rotations. In some studies, many of neurons had bilateral or ipsilateral receptive fields (42–52%; Duffy and Burchfield 1971; Sakata et al. 1973) and in other studies, most neurons had

contralateral receptive fields with only a small percentage of neurons (~8%) having bilateral or ipsilateral receptive fields (Mountcastle et al. 1975). Finally, 11% of neurons were active when the animal reached its arm or manipulated an object with his hand (Mountcastle et al. 1975). Iwamura et al. (1994, 2002) and Taoka et al. (1998, 2000) recorded from a similar location in awake animals, but also recorded further medially, in and around the postcentral sulcus (Fig. 2D,E,G). These investigators described not only neurons associated with the forelimb in area 5 but were the first to describe neurons associated with the hindlimb (Iwamura et al. 1994, 2002; Taoka et al. 1998, 2000) and proposed a topographic organization of area 5 that mirrors that of area 2. However, the hindlimb region of area 5 described by these investigators was more medial and rostral than in previous studies, in and immediately posterior to the PCS (Fig. 2E,G). This is the location of the hindlimb and trunk representation described for area 2 by Pons et al. (1985a, 1985b) (Fig. 9). As in earlier studies, they found neurons responsive mostly to stimulation of deep tissue and demonstrate that about 20% of neurons had bilateral receptive fields, with the majority located on the trunk (Taoka et al. 1998).

There are other studies that recorded from BA5 in awake animals, but as in the studies described above, the location of recording sites along the IPS varied (see Fig. 2), as did neural response properties, indicating that BA5 is composed of several different functional areas. For example, Snyder et al. (1997, 1998, 2000) found what they term a reach region, located in a far medial location in the IPS, which is involved in the generation of intended visually guided arm movements. This portion of area 5 has subsequently been termed the parietal reach region (PPR, see below). Other investigators have explored a middle portion of BA5 on the rostral bank of the IPS (e.g., Lacquaniti et al. 1995; Klam and Graf 2006; Fig. 2J). While several investigators term this field MIP, others argue that this is a portion of the PRR, which also includes other functional zones (e.g., Cohen and Andersen 2002; Grefkes and Fink 2005). Finally, Gardner, Babu, Ghosh, et al. (2007), Gardner, Babu, Reitzen, et al. (2007), and Chen et al. (2009) recorded from a very lateral portion of BA5 while monkeys were performing a reach/grasp/lift task and found that neurons appear to be involved in aspects of grasping an object.

Our results from neurons in the lateral portion of BA 5 (area 5L), including the preponderance of receptive fields on the hand and forelimb, the submodality, and receptive field laterality and configuration, are consistent with previous studies where passive stimulation was applied in either awake or anesthetized animals in a location similar to portions of area 5L (e.g., Sakata et al. 1973; Mountcastle et al. 1975; Pons et al. 1985a, 1985b). Although in one case, we observed 2 recording sites with receptive fields on the hindlimb, the location of these sites was in a medial portion of the IPS, in the presumptive area MIP, rather than in and around the PCS in area 2, or laterally in area 5L. Furthermore, our results from neurons recorded within the presumptive MIP are similar to previous investigations in awake animals in which neurons in MIP responded to passive somatic stimulation of the forelimb as well as visual and sometimes bimodal stimulation (e.g., Colby and Duhamel 1991, 1996). However, it should be noted that as in area 5L, responsiveness of neurons in this medial region to both visual and somatic stimulation can be affected by anesthetic state. The differences between studies in which different locations within BA5 were explored indicate that BA5 consists of

multiple functional fields involved in different aspects of intended manual behavior. Thus, it seems critical that the terminology regarding BA5 be altered to more appropriately reflect which portion of this large architectonic zone is being studied.

Area 5 in New World Monkeys

Full maps of area 5 have been described for New World titi (Padberg et al. 2005) and cebus monkeys (Padberg et al. 2007) and there are both common features of organization as well as differences between these primates and macaques. Area 5 in titi is located in the lateral portion of the IPS and contains neurons that respond mostly to stimulation of muscles and joints, but a subset of neurons respond to cutaneous stimulation. Like macaque monkeys, neurons in this region have large and complex receptive fields, and the representation is dominated by the hand and shoulder, although a small representation of the face was identified in one case. In titi monkeys, as in macaque monkeys, there is a gross topographic organization of the forelimb representation from proximal to distal and from medial to lateral. Furthermore, in titi monkeys, multiple representations of the same body parts are observed, resulting in a fractured map of area 5. On the other hand, compared with the macaque monkey, in titi monkeys relatively more neurons in area 5 respond to visual stimulation, and parietal cortex in general appears to be more primitive, with area 5 located immediately caudal to area 1 and no area 2 appears to be present (Padberg et al. 2005).

Although cebus monkeys are more closely related to titi monkeys than macaque monkeys, the organization, location, and extent of the area 5 identified in cebus looks more like that of the macaque than titi monkeys (Padberg et al. 2007), possibly due to the independent evolution of an opposable thumb and precision grip. As in macaque monkeys, in cebus monkeys area 5 is located immediately caudal to area 2, there is an enormous magnification of the forelimb, little or no responsiveness to visual stimulation, and neurons have multiple body part receptive fields as well as multiple representations of the same body part leading to fractured maps. However, in cebus monkeys, more neurons are responsive to cutaneous stimulation. Interestingly, in all 3 of these nonhuman primate species, there were greater individual differences in map organization in area 5 than in areas 2 and 1. Thus, in nonhuman primates, overall organizational features of area 5 appear to be similar across species, with some species-specific distinctions.

Function of Area 5L and Cortex Medial to Area 5

One of the most important features of area 5 described in early studies in awake animals was that most neurons were active when the animal actively rotated a joint and that some of the neurons, termed arm projection and hand manipulation neurons (Mountcastle et al. 1975) were active when the animal reaches its arm or manipulates an object with its hand. Mountcastle proposed that these conditional neurons provided commands for movement rather than actual instructions of how to move. Subsequent single unit recording studies in awake animals (Kalaska et al. 1990) report that neurons in area 5 were unaffected by the load conditions of a task and like Mountcastle et al. (1975) concluded that area 5 neurons encode invariant spatial parameters of a movement or movement directions. They also proposed that neurons in this

region provide a context or a point of reference for an arm movement.

More recent studies indicate that area 5L neurons are involved in coordinating or programming intention of movement (Debowy et al. 2001) and in the kinematics of acquisition (e.g., spatiotemporal coordinates) rather than the kinetics (e.g., load and force of muscle) of reaching (Kalaska 1996; Wise et al. 1997). Studies that examine the activity of neurons in 5L during the performance of a reach-grasp-lift task indicate that these neurons fire maximally before the object is contacted and decline after the object is acquired (Gardner, Babu, Reitzen, et al. 2007). Interestingly, these investigators reported that a large proportion of neurons encountered in area 5L increased their rate of firing as the fingers were preshaped just before grasping, a property also associated with the anterior intraparietal area (AIP). In a companion study (Gardner, Babu, Ghosh, et al. 2007), these investigators demonstrated that object size and hand posture affected firing rates of neurons in area 5L and that neurons in area 5L fired before those in anterior parietal fields (including area 2), which were most active during object contact or grasping of the object (Gardner, Ro, et al. 2007). They propose that neurons in area 5L coordinate reaching and grasping actions as the hand arrives at a target and that neurons in area 5L are involved in both the planning and the execution of a movement (Gardner, Babu, Reitzen, et al. 2007). Recently, they demonstrated that most neurons in the rostral portion of area 5L modulate their firing rate based on the approach style and that there was a strong correlation between approach style and object properties such as size and shape (Chen et al. 2009), thus coordinating the arm and hand for reaching and grasping.

The terminology used to define cortex medial to area 5L differs in that some studies refer to this as area 5 (e.g., Ferraina and Bianchi 1994; Lacquaniti et al. 1995), some term this the parietal reach region (PRR; e.g., Calton et al. 2002; Scherberger et al. 2003; Chang et al. 2008), some studies refer to this general region as the medial intraparietal area (MIP; e.g., Colby and Duhamel 1991, 1996; Eskandar and Assad 2002; Mullette-Gillman et al. 2005, Fig. 2; Klam and Graf 2006; Durand et al. 2007; Compare Fig. 1 of Scherberger et al. 2003 with Fig. 1 of Klam and Graf 2006; Fig. 12), and some studies distinguish area 5 and MIP as separate fields rather than incorporating MIP into the larger architectonic zone of BA5 (e.g., Johnson et al. 1996). Because of these issues, making comparisons across studies, including the present one, is problematic.

Not surprisingly, differences in terminology and location of recording in medial portions of the IPS have led to differences in what is considered to be the function of this region. For example, some studies suggest that neurons in this region (termed PRR) are involved in planning contralateral limb movements and transforming visual information regarding target location into a plan for visually guided reaching (Cohen and Andersen 2002; Chang et al. 2008; Chang and Snyder 2010). Some studies indicate that neurons in a similar location, but termed MIP, are responsive to vestibular stimulation (passive head rotations) and that these neurons discriminate active versus passive head movement, are involved in self-motion perception and coordination of movements in space and time (Klam and Graf 2006). Other studies demonstrate that neurons in this medial region are directionally selective to hand movement and integrate hand-related directional information with goal related information (Eskandar and Assad 2002), quite similar to the recent proposition of Chang et al. (2008) for

neurons in PRR. Finally, some studies propose that this region (area 5) is generating body or shoulder-centered (rather than eye-centered) coordinates for reaching (Ferraina and Bianchi 1994; Lacquaniti et al. 1995).

While there are differences in the proposed function of portions of architectonically defined area 5, most studies implicate the medial portion of the IPS in translating and combining multiple frames of reference (gaze centered, body centered, head centered) into a common coordinate system or integrated plan for reaching toward an intended target in immediate extra personal space (Buneo et al. 2002). The lateral portion of the IPS, area 5L, appears to be involved in the kinematics of reaching, coordinating multiple limb parts for reaching and grasping actions, and matching object properties, such as size and shape, with grasping configurations. Our data support these findings by demonstrating a preponderance of contralateral receptive fields in area 5L, a large magnification of the forelimb, complex multi joint receptive fields, and a fractured map of body parts that constitutes related groups of proprioceptors activated during behaviorally relevant movements.

Supplementary Material

Supplementary material can be found at: <http://www.cercor.oxfordjournals.org/>

Funding

This work was supported by the National Institute of Neurological Disorders and Stroke (R01NS035103-13A1 to L.K.) and in part by National Institutes of Health grants (T32 DC8072 to A.S., F32NS064792 to A.S., and F32EY014503 to J.P.).

Notes

Conflict of Interest: None declared.

References

- Bisley JW, Goldberg ME. 2010. Attention, intention, and priority in the parietal lobe. *Annu Rev Neurosci.* 33:1-21.
- Britten KH. 2008. Mechanisms of self-motion perception. *Annu Rev Neurosci.* 31:389-410.
- Brodman K. 1909. *Vergleichende Lokalisationslehre der Grobhirnrinde.* Leipzig (Germany): Barth.
- Buneo CA, Jarvis MR, Batista AP, Andersen RA. 2002. Direct visuomotor transformations for reaching. *Nature.* 416:632-636.
- Calton JL, Dickinson AR, Snyder LH. 2002. Non-spatial, motor-specific activation in posterior parietal cortex. *Nat Neurosci.* 5:580-588.
- Caminiti R, Chafee MV, Battaglia-Mayer A, Averbach BB, Crow DA, Georgopoulos AP. 2010. Understanding the parietal lobe syndrome from a neurophysiological and evolutionary perspective. *Eur J Neurosci.* 31:2310-2010.
- Carroll EW, Wong-Riley MTT. 1984. Quantitative light and electron microscopic analysis of cytochrome oxidase-rich zones in the striate cortex of the squirrel monkey. *J Comp Neurol.* 222:1-17.
- Chang SW, Dickinson AR, Snyder LH. 2008. Limb-specific representation for reaching in the posterior parietal cortex. *J Neurosci.* 28:6128-6140.
- Chang SW, Snyder LH. 2010. Idiosyncratic and systematic aspects of spatial representations in the macaque parietal cortex. *Proc Natl Acad Sci U S A.* 107:7951-7956.
- Chen J, Reitzen S, Kohlenstein J, Gardner E. 2009. Neural representation of hand kinematics during prehension in posterior parietal cortex of the macaque monkey. *J Neurophysiol.* 102:3310-3328.

- Cohen YE, Andersen RA. 2002. A common reference frame for movement plans in the posterior parietal cortex. *Nat Rev Neurosci*. 3:553-562.
- Colby CL, Duhamel JR. 1991. Heterogeneity of extrastriate visual areas and multiple parietal areas in the macaque monkey. *Neuropsychologia*. 29:517-537.
- Colby CL, Duhamel JR. 1996. Spatial representations for action in parietal cortex. *Cogn Brain Res*. 5:105-115.
- Darian-Smith C, Darian-Smith I. 1993. Thalamic projections to areas 3a, 3b, and 4 in the sensorimotor cortex of the mature and infant macaque monkey. *J Comp Neurol*. 335:173-199.
- Debowy DJ, Ghosh S, Ro JY, Gardner EP. 2001. Comparison on neuronal firing rates in somatosensory and posterior parietal cortex during prehension. *Exp Brain Res*. 137:269-291.
- Duffy FH, Burchfield JL. 1971. Somatosensory system: organizational hierarchy from single units in monkey area 5. *Science*. 172:273-275.
- Durand JB, Nelissen K, Joly O, Wardak C, Todd JT, Norman JF, Janssen P, Vanduffel W, Orban GA. 2007. Anterior regions of monkey parietal cortex process visual 3D shape. *Neuron*. 55:493-505.
- Eskandar EN, Assad JA. 2002. Distinct nature of directional signals among parietal cortical areas during visual guidance. *J Neurophysiol*. 88:1777-1790.
- Ferraina S, Bianchi L. 1994. Posterior parietal cortex: functional properties of neurons in area 5 during an instructed-delay reaching task within different parts of space. *Exp Brain Res*. 99:175-178.
- Gallyas F. 1979. Silver staining of myelin by means of physical development. *Neurology*. 1:203-209.
- Gardner EP, Babu KS, Ghosh S, Sherwood A, Chen J. 2007. Neurophysiology of prehension. III. Representation of object features in posterior parietal cortex of the macaque monkey. *J Neurophysiol*. 98:3708-3730.
- Gardner EP, Babu KS, Reitzen SD, Ghosh S, Brown AS, Chen J, Hall AL, Herzlinger MD, Kohlenstein JB, Ro JY. 2007. Neurophysiology of prehension. I. Posterior parietal cortex and object-oriented hand behaviors. *J Neurophysiol*. 97:387-406.
- Gardner EP, Ro JY, Babu KS, Ghosh S. 2007. Neurophysiology of prehension. II. Response diversity in primary somatosensory (S-1) and motor (M-1) cortices. *J Neurophysiol*. 97:1656-1670.
- Gould HJ, 3rd, Cusick CG, Pons TP, Kaas JH. 1986. The relationship of corpus callosum connections to electrical stimulation maps of motor, supplementary motor, and the frontal eye fields in owl monkeys. *J Comp Neurol*. 247:297-325.
- Grefkes C, Fink GR. 2005. The functional organization of the intraparietal sulcus in humans and monkeys. *J Anat*. 207:3-17.
- Hof PR, Morrison JH. 1995. Neurofilament protein defines regional patterns of cortical organization in the macaque monkey visual system: a quantitative immunohistochemical analysis. *J Comp Neurol*. 352:161-186.
- Hyvärinen J, Poranen A. 1978. Receptive field integration and submodality convergence in the hand area of the post-central gyrus of the alert monkey. *J Physiol*. 283:539-556.
- Iwamura Y, Iriki A, Tanaka M. 1994. Bilateral hand representation in the postcentral somatosensory cortex. *Nature*. 369:554-556.
- Iwamura Y, Tanaka M, Iriki A, Taoka M, Toda T. 2002. Processing of tactile and kinesthetic signals from bilateral sides of the body in the postcentral gyrus of awake monkeys. *Behav Brain Res*. 135:185-190.
- Johnson PB, Ferraina S, Bianchi L, Caminiti R. 1996. Cortical networks for visual reaching: physiological and anatomical organization of frontal and parietal lobe arm regions. *Cereb Cortex*. 6:102-119.
- Kaas JH. 1982. The segregation of function in the nervous system: why do the sensory systems have so many subdivisions? *Contrib Sens Physiol*. 7:201-240.
- Kalaska JF. 1996. Parietal cortex area 5 and visuomotor behavior. *Can J Physiol Pharmacol*. 74:483-498.
- Kalaska JF, Cohen DA, Prud'homme M, Hyde ML. 1990. Parietal area 5 neuronal activity encodes movement kinematics, not movement dynamics. *Exp Brain Res*. 80:351-364.
- Klam F, Graf W. 2006. Discrimination between active and passive head movements by macaque ventral and medial intraparietal cortex neurons. *J Physiol*. 574:367-386.
- Krubitzer L, Disbrow E. 2008. The evolution of parietal areas involved in hand use in primates. In: Gardner E, Kaas JH, editors. *The senses: a comprehensive references*. London: Elsevier. p. 183-214.
- Krubitzer LK. 2009. In search of a unifying theory of complex brain evolution. *Ann N Y Acad Sci*. 1156:44-67.
- Krubitzer LA, Huffman KJ, Disbrow E, Recanzone GH. 2004. Organization of area 3a in macaque monkeys: contributions to the cortical phenotype. *J Comp Neurol*. 471:97-111.
- Lacquaniti F, Guigon E, Bianchi L, Ferraina S, Caminiti R. 1995. Representing spatial information for limb movement: the role of area 5 in monkey. *Cereb Cortex*. 5:391-409.
- Lewis JW, Van Essen DC. 2000. Mapping of architectonic subdivisions in the macaque monkey, with emphasis on parieto-occipital cortex. *J Comp Neurol*. 428:79-111.
- Mountcastle VB, Lynch JC, Georgopoulos A, Sakata H, Acuña C. 1975. Posterior parietal association cortex of the monkey: command functions for operations within extrapersonal space. *J Neurophysiol*. 38:871-908.
- Mullette-Gillman OA, Cohen YE, Groh JM. 2009. Motor-related signals in the intraparietal cortex encode locations in a hybrid, rather than eye-centered reference frame. *Cereb Cortex*. 19:1761-1775.
- Nelson RJ, Sur M, Felleman DJ, Kaas JH. 1980. Representations of the body surface in postcentral parietal cortex of *Macaca fascicularis*. *J Comp Neurol*. 192:611-643.
- Padberg J, Cerkevich C, Engle J, Rajan AT, Recanzone G, Kaas J, Krubitzer L. 2009. Thalamocortical connections of parietal somatosensory cortical fields in macaque monkeys are highly divergent and convergent. *Cereb Cortex*. 19:2038-2064.
- Padberg J, Disbrow E, Krubitzer L. 2005. The organization and connections of anterior and posterior parietal cortex in titi monkeys: do New World monkeys have an area 2? *Cereb Cortex*. 15:1938-1963.
- Padberg J, Franca J, Cooke D, Soares J, Rosa M, Fiorani M, Gattass R, Krubitzer L. 2007. Parallel evolution of cortical areas involved in skilled hand use. *J Neurosci*. 27:10106-10115.
- Padberg J, Recanzone G, Engle J, Cooke D, Goldring A, Krubitzer L. 2010. Lesions in posterior parietal area 5 in monkeys result in rapid behavioral and cortical plasticity. *J Neurosci*. 30:12918-12935.
- Pons TP, Garraghty PE, Cusick CG, Kaas JH. 1985a. A sequential representation of the occiput, arm, forearm and hand across the rostrocaudal dimension of areas 1,2 and 5 in macaque monkeys. *Brain Res*. 335:350-353.
- Pons TP, Garraghty PE, Cusick CG, Kaas JH. 1985b. The somatotopic organization of area 2 in macaque monkeys. *J Comp Neurol*. 241:445-466.
- Remple MS, Reed JL, Stepniewska I, Kaas JH. 2006. Organization of frontoparietal cortex in the tree shrew (*Tupaia belangeri*). I. Architecture, microelectrode maps, and corticospinal connections. *J Comp Neurol*. 497:133-154.
- Rothmund Y, Qi H-X, Collins CE, Kaas JH. 2002. The genitals and gluteal skin are represented lateral to the foot in anterior parietal somatosensory cortex of macaques. *Somatosens Mot Res*. 19:302-315.
- Roy AC, Stefanini S, Pavesi G, Gentilucci M. 2004. Early movement impairments in a patient recovering from optic ataxia. *Neuropsychologia*. 42:847-854.
- Sakata H, Takaoka Y, Kawarasaki A, Shibutani H. 1973. Somatosensory properties of neurons in the superior parietal cortex (area 5) of the rhesus monkey. *Brain Res*. 64:85-102.
- Scherberger H, Fineman I, Musallam S, Dubowitz DJ, Bernheim KA, Pesaran B, Corneil BD, Gilliken B, Andersen RA. 2003. Magnetic resonance image-guided implantation of chronic recording electrodes in the macaque intraparietal sulcus. *J Neurosci Methods*. 130:1-8.
- Seltzer B, Pandya DN. 1986. Posterior parietal projections to the intraparietal sulcus of the rhesus monkey. *Exp Brain Res*. 62:459-469.
- Snyder LH, Batista AP, Andersen RA. 1997. Coding of intention in the posterior parietal cortex. *Nature*. 386:167-170.
- Snyder LH, Batista AP, Andersen RA. 1998. Change in motor plan, without a change in the spatial locus of attention, modulates activity in posterior parietal cortex. *J Neurophysiol*. 79:2814-2819.
- Snyder LH, Batista AP, Andersen RA. 2000. Saccade-related activity in the parietal reach region. *J Neurophysiol*. 83:1099-1102.

- Stepniewska I, Preuss TM, Kaas JH. 1993. Architectonics, somatotopic organization, and ipsilateral cortical connections of the primary motor area (M1) of owl monkeys. *J Comp Neurol.* 330:238-271.
- Taoka M, Toda T, Iriki A, Tanaka M, Iwamura Y. 2000. Bilateral receptive field neurons in the hindlimb region of the postcentral somatosensory cortex in awake macaque monkeys. *Exp Brain Res.* 134:139-146.
- Taoka M, Toda T, Iwamura Y. 1998. Representation of the midline trunk, bilateral arms, and shoulders in the monkey postcentral somatosensory cortex. *Exp Brain Res.* 123:315-322.
- Tsutsui K-I, Taira M, Sakata H. 2005. Neural mechanisms of three-dimensional vision. *Neurosci Res.* 51:221-229.
- Trillenber P, Sprenger A, Petersen D, Kompf D, Heide W, Helmchen C. 2007. Functional dissociation of saccade and hand reaching control with bilateral lesions of the medial wall of the intraparietal sulcus: implication for optic ataxia. *Neuroimage.* 36:T69-T76.
- von Bonin G, Bailey P. 1947. *The neocortex of Macaca mulatta.* Urbana (IL): University of Illinois.
- von Economo C. 1929. *The cytoarchitectonics of the cerebral cortex.* London: Oxford University Press.
- Wise SP, Boussaoud D, Johnson PB, Caminiti R. 1997. Premotor and parietal cortex: corticocortical connectivity and combinatorial computations. *Annu Rev Neurosci.* 20:25-42.
- Wu CW, Bichot NP, Kaas JH. 2000. Converging evidence from microstimulation, architecture, and connections for multiple motor areas in the frontal and cingulate cortex of prosimian primates. *J Comp Neurol.* 423:140-177.